J. Fluid Mech. (1966), *vol.* 24, *part* 3, *pp.* 481–495
Printed in Great Britain

Laminar flow past a sphere at high Mach number

By R. T. DAVIS AND W. J. CHYU
Engineering Mechanics Department, Virginia Polytechnic Institute

(Received 15 June 1965)

Laminar hypersonic flow past a sphere is examined on the basis of the constant-density approximation. The Navier–Stokes equations governing the flow are reduced to a nearly parabolic form so that backward influence is essentially eliminated. Two methods of solution are then used on the resulting equations. The first method is the so-called series-truncation method (local similarity), and the second method is an implicit finite-difference method. The solutions from the two methods are compared for various values of the shock Reynolds number. These solutions are also compared with Lighthill's inviscid constant-density solution for high-shock Reynolds number.

1. Introduction

The high-speed flow of a compressible fluid over a blunt body at moderate to low Reynolds numbers has attracted considerable attention owing to its application to re-entry problems. The flow régime where the Reynolds number is high enough for boundary-layer theory to apply can be handled without too much difficulty. This is done by obtaining a numerical solution to the inviscid flow equations describing the flow outside the boundary layer and using this solution to obtain the pressure distribution on the body surface. One can then use this pressure distribution to solve the boundary-layer equations by one of several methods available such as those of Flügge-Lotz & Blottner (1962), Smith & Clutter (1963), and Davis & Flügge-Lotz (1964). (The last method is actually a modification of the method of Flügge-Lotz & Blottner.) Boundary-layer calculations have been made for several flow cases by using the above methods. In particular one is referred to the hypersonic blunt-body solutions by Davis & Flügge-Lotz (1964).

At lower Reynolds numbers one must contend with the fact that the first-order boundary-layer equations cannot be expected to give reasonable results. This can be corrected at the high Reynolds number end by solving the so-called second-order boundary-layer equations. This has also been done by Davis & Flügge-Lotz (1964). This, however, becomes quite cumbersome and requires a considerable amount of computing time. If one needs to go to third-order boundary-layer theory for sufficient accuracy the situation would be even more difficult. One of the difficulties encountered is the problem of calculating the flow due to displacement thickness. This requires a direct solution for the inviscid flow past a body consisting of the original body thickened by the displacement thickness. Davis & Flügge-Lotz (1964) approximated this flow by shifting and expanding the original body surface. Hoffman (1964) has approached the problem in a more exact manner by using the method of integral relations to calculate the flow field. Neither method is entirely satisfactory, the first because of inaccuracy and the second because of computational difficulties. Another difficulty with higher-order boundary layer theory is the fact that at moderate Reynolds numbers the boundary-layer begins to spread into the entire shock layer, preventing one from clearly distinguishing separate inviscid and viscous regions (see Kao 1964) and therefore limiting boundary-layer theory to higher Reynolds numbers than one might expect.

For the reasons above one is presented with the idea of trying to solve the complete Navier–Stokes equations or a simplification of them which is valid in the whole shock layer. Davis & Flügge-Lotz (1964) have suggested such a simplification and a method for solving their simplified equations. The purpose of this paper is to present the results of an investigation which uses the method suggested by Davis & Flügge-Lotz (1964).

For simplicity we shall consider the constant-density flow past a sphere. There are several reasons for this. Firstly, an exact inviscid solution for the inviscid part of the flow field in the high-Reynolds-number flows is available for comparison due to Lighthill (1957). Secondly, the constant-density model will retain all the essential features for the numerical procedure of the solution of flow for the more complicated compressible fluid. Once the constant-density case has been solved the extension to the compressible case is direct, with no complications arising due to theory. For simplicity we shall also assume that the shock is a discontinuity even in the low-Reynolds-number cases. This is again a simplification which can be removed (see Cheng 1963).

In order to start the numerical procedure one must have a solution which is valid near the stagnation point. The ideal method for finding this solution is to use the series-truncation method developed by Van Dyke and co-workers. In particular the truncated-series method used by Kao (1964) in the compressible viscous flow past a sphere is useful. The truncated-series results should be particularly good since the form of the truncation is taken to be the same as the form of the inviscid constant-density solution. These results are also used for comparison with the numerical finite-difference results.

For the purpose of comparison with the high-Reynolds-number cases the first-order boundary-layer equations are also solved for the constant-density flow. In this case Lighthill's (1957) constant-density solution is used for determining the surface-pressure distribution.

2. Formulation of the problem

2.1. *Co-ordinate system*

Consider laminar hypersonic flow of a viscous fluid past the sphere of radius a^* shown in figure 1. For simplicity we shall assume that the free-stream Mach number M_∞ is infinite and that the density ρ_s^* and viscosity μ_s^* in the flow field behind the shock are constants given by their values immediately behind the normal shock. The velocity components u^* and v^* are tangent and normal to the body surface respectively. The co-ordinate n^*, is measured normal to the body surface and the angle ϕ is measured from the stagnation point to the radius vector.

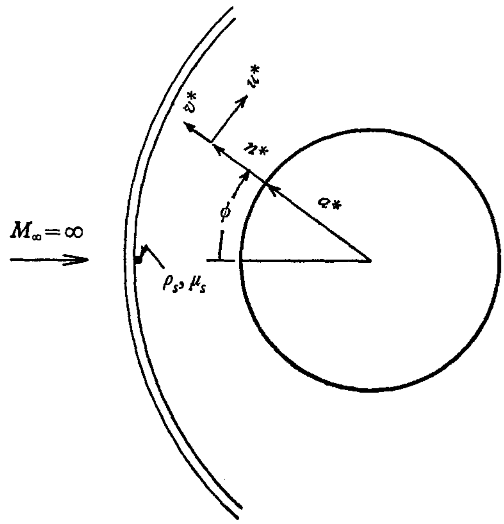

FIGURE 1. Co-ordinate system.

2.2. *Dimensionless quantities*

For simplicity the following dimensionless quantities are introduced. These quantities are of order one in the boundary-layer region near the surface of the sphere.

$$N = n^*/\tau a^*, \text{ boundary-layer normal co-ordinate,} \tag{2.1a}$$

$$a = a^*/a^* = 1, \text{ nose radius,} \tag{2.1b}$$

$$u = u^*/U^*_\infty, \text{ the velocity component parallel to the body surface,} \tag{2.1c}$$

$$P = P^*/\rho^*_\infty U^{*2}_\infty, \text{ the pressure,} \tag{2.1d}$$

$$\rho_s = \rho^*_s/\rho^*_\infty = 6, \text{ the density behind the shock for } M_\infty = \infty. \tag{2.1e}$$

$$(\tau_f)_w = (\tau^*_f)_w \sqrt{Re_s}/\rho^*_\infty U^{*2}_\infty = \partial u/\partial N, \text{ shear stress at the body surface,} \tag{2.1f}$$

$$Re_s = U^*_\infty a^* \rho^*_\infty/\mu^*_s, \text{ shock Reynolds number.} \tag{2.1g}$$

The quantity τ used in the above relations is defined by

$$\tau = 1/\sqrt{Re_s}. \tag{2.1h}$$

2.3. *Assumptions*

We shall assume that the constant-density model is applicable. This will be true near the stagnation point for a nearly insulated body. We shall further assume that the no-slip conditions apply at the body surface. These conditions can be modified with little difficulty to take care of slip (see Street 1960). We shall also assume that the bow shock wave is a discontinuity even though this is not true at low Reynolds numbers. This restriction can be removed in a manner similar to that of Cheng (1963). All these restrictions are imposed to allow attention to be focused on the numerical procedure. The restrictions of constant density, no slip, etc., can be removed with little change in the method of solution. These more general calculations, which conform more closely with the real situation, are being made at present.

The last assumption is that the angles of inclination of the bow shock wave and a tangent drawn to the body surface are the same for a given value of ϕ. This is similar to assuming a spherical shock except that the distance between the body and the shock is allowed to grow. Since the shock is spherical in the inviscid case this assumption is very good for high Reynolds numbers. On the basis of the numerical calculations we shall see that this is not a bad assumption even at low Reynolds numbers. We have tried to build up the shock wave in the viscous case as the computations proceed downstream; however, this has led to instabilities in the numerical procedure. This point is under study at present and an attempt is being made to impose the shock conditions in such a way that instabilities do not occur. This difficulty must be overcome before other body shapes are considered along with a compressible fluid.

Assumptions similar to some of those made above (i.e. constant density etc.) have been made by Probstein & Kemp (1960), Oguchi (1958), and Hoshizaki (1959) in considering the viscous flow past a sphere.

2.4. *Governing equations and boundary conditions*

Introducing the dimensionless quantities (2·1*a*)–(2.1*g*) into the full Navier–Stokes equations and neglecting all terms of higher than second order in Reynolds number, which appear in both the boundary-layer region near the body and also in the inviscid region outside this layer, we can obtain a set of equations similar to those given by Davis & Flügge-Lotz (1964). (See their paper for a discussion of this approximation.) On making the constant-density approximation we obtain the following set of partial-differential equations and boundary conditions:

Continuity†

$$[\{(1+\tau N)\sin\phi\}\,u]_\phi+[(1+\tau N)\{(1+\tau N)\sin\phi\}\,v]_N=0; \tag{2.2a}$$

ϕ-Momentum

$$\rho_s\left(\frac{uu_\phi}{1+\tau N}+vu_N+\frac{\tau}{1+\tau N}uv\right)+\frac{P_\phi}{1+\tau N}=u_{NN}+\frac{2\tau}{1+\tau N}u_N; \tag{2.2b}$$

N-Momentum

$$\rho_s\left(\frac{\tau uv_\phi}{1+\tau N}+\tau vv_N-\frac{u^2}{1+\tau N}\right)+\frac{1}{\tau}P_N=0; \tag{2.2c}$$

Surface conditions

$$u,v=0\quad\text{at}\quad N=0; \tag{2.2d}$$

Shock conditions (*spherical*, $M_\infty=\infty$)

$$P_s=\frac{2}{\gamma+1}-\frac{2}{\gamma+1}\sin^2\phi, \tag{2.2e}$$

$$u_s=\sin\phi, \tag{2.2f}$$

$$v_s=-\frac{1}{\tau}\frac{(\gamma-1)}{(\gamma+1)}\cos\phi. \tag{2.2g}$$

† Subscripts s denote conditions behind the normal shock and subscripts ϕ and N denote differentiation.

The position of the shock will be located by the requirement that the conditions (2.2*e*)–(2.2*g*) above be satisfied. In addition, total mass conservation between the body and the shock is checked by the condition that

$$(1+\tau N_s)^2 \sin\phi = 2\tau\rho_s \int_0^{N_s} u(1+\tau N)\,dN. \tag{2.2h}$$

The value of N_s at which this condition is satisfied can also be used to determine the shock position.

3. Methods of solution of the governing equation

3.1. *Series truncation method*

In order to start the numerical finite-difference method it is necessary to have an accurate solution for the flow near the stagnation point. The series-truncation method developed and applied by Van Dyke and co-workers is ideal for doing this. In the constant-density flow past a sphere it is obvious that the form that one should take for the truncation is the form of the constant-density inviscid solution of Lighthill (1957). This should be particularly accurate in the high-Reynolds-number range when the boundary layer is thin and the shock is nearly spherical. The form of the truncation used by Kao (1964) for the compressible case is exactly the same as the form which will be used here. Probstein & Kemp (1960) and other authors have made similar truncations in solving the same problem of constant-density flow past a sphere.

Assume

$$P(N,\phi) = P_1(N) + P_2(N)\sin^2\phi + \ldots, \tag{3.1a}$$

$$u(N,\phi) = u_1(N)\sin\phi + \ldots, \tag{3.1b}$$

$$v(N,\phi) = -v_1(N)\cos\phi + \ldots. \tag{3.1c}$$

Substituting these expressions into the continuity and momentum equations (2.2*a*)–(2.2*c*) and collecting terms, we obtain the following set of ordinary differential equations,

$$(1+\tau N)\,v_{1N} - 2(u_1 - \tau v_1) = 0, \tag{3.2a}$$

$$u_{1NN} + \left(\rho_s v_1 + \frac{2\tau}{1+\tau N}\right) u_{1N} - \rho_s \frac{u_1^2}{1+\tau N} + \rho_s \frac{\tau u_1 v_1}{1+\tau N} - \frac{2P_2}{1+\tau N} = 0, \tag{3.2b}$$

$$P_{2N} - \tau\rho_s \left(\frac{u_1^2}{1+\tau N} + \tau v_1 v_{1N} - \frac{\tau u_1 v_1}{1+\tau N}\right) = 0, \tag{3.2c}$$

$$P_{1N} - \tau^2 \rho_s v_1 v_{1N} = 0. \tag{3.2d}$$

The corresponding surface and shock conditions are:

At the body

$$u_1, v_1 = 0 \quad \text{at} \quad N = 0; \tag{3.2e}$$

At the shock (*spherical*, $M_\infty = \infty$)

$$v_{1s} = \frac{1}{\tau}\frac{\gamma-1}{\gamma+1}, \tag{3.2f}$$

$$u_{1s} = 1, \tag{3.2g}$$

$$P_{2s} = -2/(\gamma+1), \tag{3.2h}$$

$$P_{1s} = 2/(\gamma+1). \tag{3.2i}$$

Finally, conservation of mass requires that

$$(1+\tau N_s)^2 = 2\tau\rho_s \int_0^{N_s} u_1(1+\tau N)\,dN. \tag{3.2j}$$

It should be noted that the first three differential equations (3.2*a*)–(3.2*c*) do not involve P_1 and can therefore be solved independently of P_1. After the solution is obtained, P_1 can be determined from equation (3.2*d*).

The set of equations (3.2*a*)–(3.2*c*) is fourth-order. Only two boundary conditions are given at the body surface ($N = 0$). The method of solution is to guess values for P_2 and u_{1N} at the body surface and then to integrate numerically, starting from the body surface. Good initial guesses can be made for P_2 and u_{1N} on the basis of boundary-layer theory. Lighthill's (1957) inviscid constant-density solution along with one term of the Blasius series expansion for the boundary-layer equations near the stagnation point provide a fairly good initial guess, even in the low-Reynolds-number cases. The integration is carried out until the shock condition on u_1 is satisfied. Values of v_1 and P_2 will then be determined. Interpolation using Newton's method will allow the shock conditions on v_1 and P_2 to be satisfied after a few tries. It was found that mass-conservation equation (3.2*j*) was satisfied to sufficient accuracy.

The numerical scheme used was the Runge–Kutta–Gill method on an I.B.M. 7040 electronic digital computer. Each integration required less than 1 min computing time, and sufficient accuracy was assured by halving the step size until no change in the results was noted in the first four decimal places. The numerical results were carried out for values of Re_s of 900, 100, and 49 ($\tau = \frac{1}{30}, \frac{1}{10}$, and $\frac{1}{7}$). The results of these computations will be discussed later along with the results from the finite-difference method. The results are in agreement with those of Probstein & Kemp (1960).

3.2. *Finite-difference method*

The main simplification is to reduce the Navier–Stokes equations governing the fluid motion to a set of parabolic partial differential equations so that backward influence is eliminated, and so that integration can be performed by starting from the stagnation point and integrating downstream along the body surface. The first step in doing this is to use the simplified form of the Navier–Stokes equations (2.2*a*)–(2.2*c*) which retain only terms up to second-order for large Reynolds number. The significance of these equations as far as numerical integration is concerned has been discussed by Davis & Flügge-Lotz (1964). (A similar set of equations has been used by Cheng 1963.) The method of solution used is similar to the implicit finite-difference method developed by Flügge-Lotz & Blottner (1962) for solving the boundary-layer equations. For details of the method one is referred to Flügge-Lotz & Blottner (1962) and Davis & Flügge-Lotz (1964).

A three-point backward difference scheme in the ϕ-direction is used for high accuracy in evaluating the derivatives in the ϕ-direction (see Davis & Flügge-Lotz 1964). In the discussion that follows no mention will be made of the differences in the N-direction, since the method for handling these is exactly the same as the method used by Flügge-Lotz & Blottner (1962) or Davis & Flügge-Lotz (1964).

The flow field between the body and the shock is overlaid with a grid of lines parallel to the N- and ϕ-co-ordinate lines, respectively. It is assumed that the spacing ($\Delta\phi$ and ΔN) between the grid lines is constant. Grid lines normal to the body surface, i.e. lines of constant ϕ, are denoted with a subscript m. It is assumed that flow quantities are known initially (from the series-truncation solution) along the grid lines $\phi = \phi_m$ and $\phi = \phi_{m-1}$. The unknown quantities are then at $\phi = \phi_{m+1} = \phi_m + \Delta\phi$. A difference equation can then be obtained from the ϕ momentum equation at the point $\phi = \phi_{m+1}$ in the same manner as that used by Davis & Flügge-Lotz (1964) on the boundary-layer equations. This difference equation is linearized by replacing non-linear quantities like $v_{m+1}(\partial u/\partial N)_{m+1}$ by $(2v_m - v_{m-1})(\partial u/\partial N)_{m+1}$. By linearizing in this manner we eliminate the unknown quantity v_{m+1} from the momentum equation. The only two remaining unknowns in that equation are then u and P. We further simplify the equation by eliminating $P_{\phi m+1}$, using the relation

$$P_{\phi m+1} = 2P_{\phi m} - P_{\phi m-1} + O(\Delta\phi^2). \tag{3.3}$$

By writing $(\partial u/\partial N)_{m+1}$, $(\partial^2 u)/\partial N^2)_{m+1}$ etc. in difference form in the N-direction, we now have an equation for the determination of u only at the station $m+1$. This involves the solution of simultaneous algebraic equations; however, the method of solution is simple and direct (see Richtmyer 1957 and Flügge-Lotz & Blottner 1962).

After u_{m+1} has been determined at all points across the shock layer v_{m+1} can be determined from the continuity equation by numerical integration. This is given by

$$v = -\left(\frac{1}{(1+\tau N)^2 \sin\phi}\right)\int_0^N [\{(1+\tau N)\sin\phi\}\, u]_\phi\, dn, \tag{3.4}$$

where all terms on the right-hand side are known and v_{m+1} can then be determined by integrating to the value of N corresponding to the grid point of interest. The derivative inside the integral is evaluated by using a three-point backward difference quotient, and the integration is then performed by using the trapezoidal or some other integration formula.

Now that v_{m+1} has been determined at all points across the shock layer at station $m+1$, we may determine P_{m+1}. This is done in the same manner as was used for v_{m+1} but by integrating the N-momentum equation. This gives

$$P = P_w + \tau\rho_s \int_0^N \left(\frac{u^2}{1+\tau N} - \frac{\tau u v_\phi}{1+\tau N} - \tau v v_{1N}\right) dN, \tag{3.5}$$

where P_w is the pressure at the body surface, and is determined by making the above equation satisfy the correct condition on pressure at the shock. It was found that, near the stagnation point, the inclusion of the second two terms of the integrand in equation (3.5) led to numerical instabilities. For this reason they were neglected in the finite-difference calculations but were then included in a second iteration in determining the pressure. This assumption is consistent with thin shock-layer theory and gives excellent agreement with the series-truncation results. The adequacy of equation (3.3) in determining the pressure gradient at the station $m+1$ was also checked by iteration at station $m+1$, and it was found that there was very little change in the results for the pressure distribution.

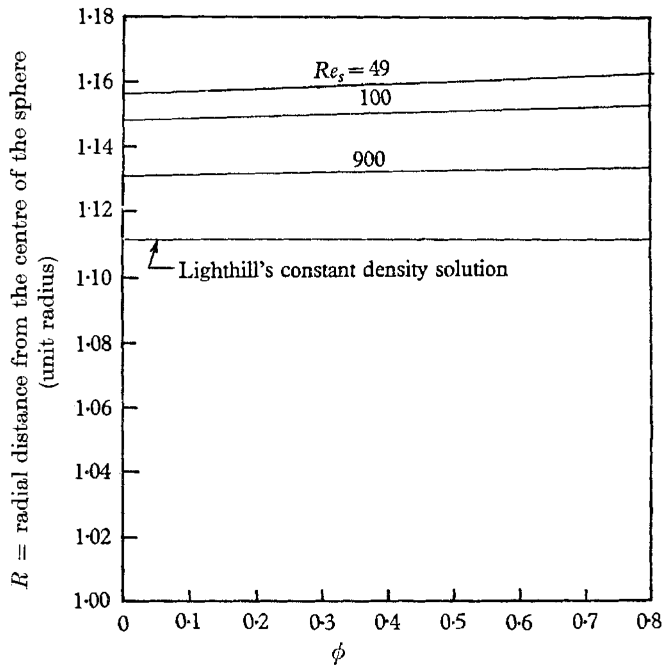

FIGURE 2. Radial distance to the shock at various Reynolds numbers.

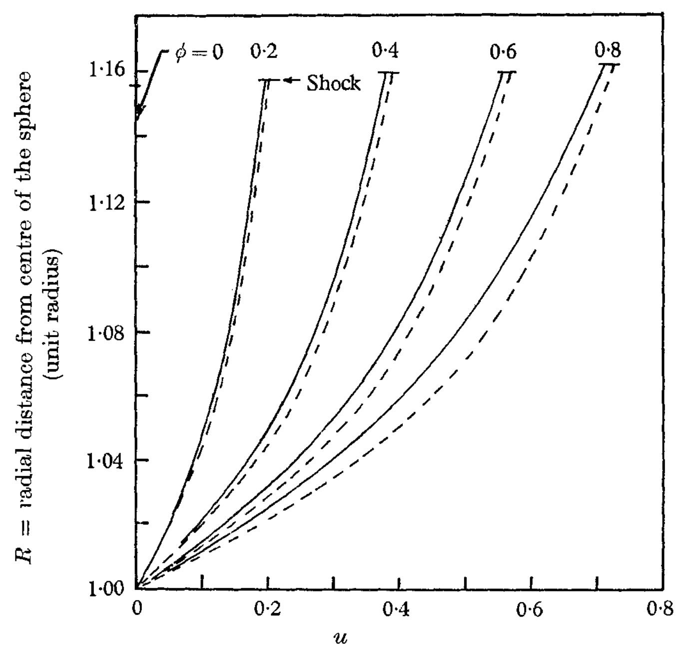

FIGURE 3(*a*). Velocity distribution in the shock layer for $Re_s = 49$. ——, Finite-difference method; – – –, truncated-series method.

Using the solution obtained in the manner above as a first step it may be possible to build up a more exact solution to the Navier–Stokes equations by an iteration procedure. This possibility is being considered at the present time in addition to the extension of the numerical method to a compressible fluid.

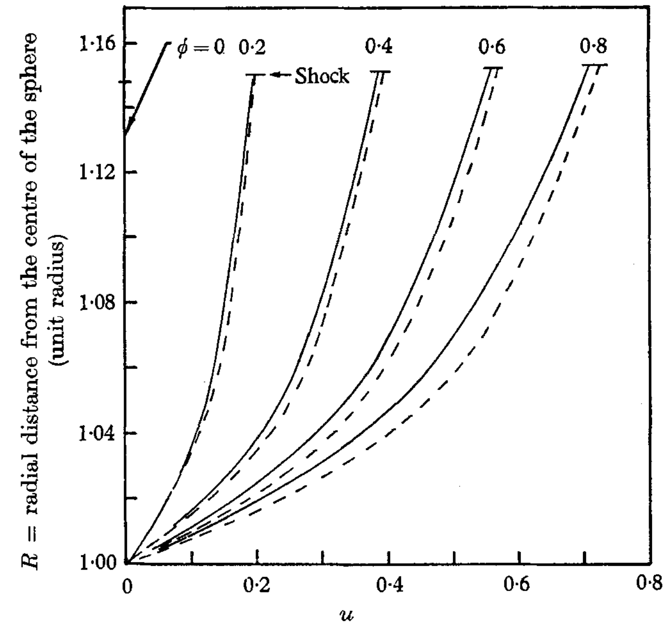

FIGURE 3(*b*). Velocity distribution in the shock layer for $Re_s = 100$. ——, Finite-difference method; – – –, truncated-series method.

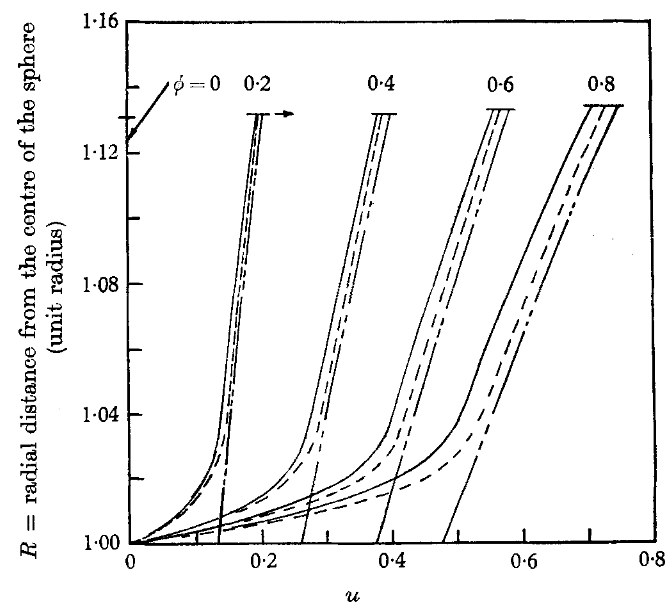

FIGURE 3(*c*). Velocity distribution in the shock layer for $Re_s = 900$. ——, Finite-difference method; – – – –, truncated-series method; —·-·— Lighthill's constant-density solution.

4. Results

The results for the solutions using both the series-truncation method and the finite-difference method are shown in figures 2–5.

Figure 2 indicates that at high Reynolds number the shock is spherical, as Lighthill's (1957) inviscid solution indicates. Even in the low-Reynolds-number

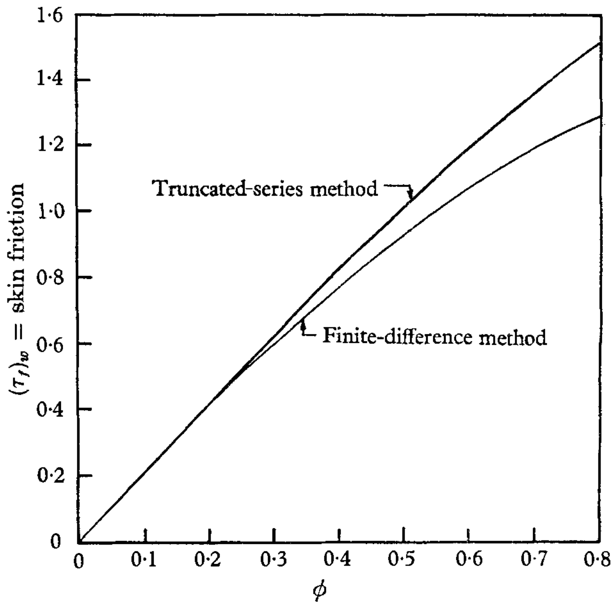

FIGURE 4(*a*). Variation of skin friction for $Re_s = 49$.

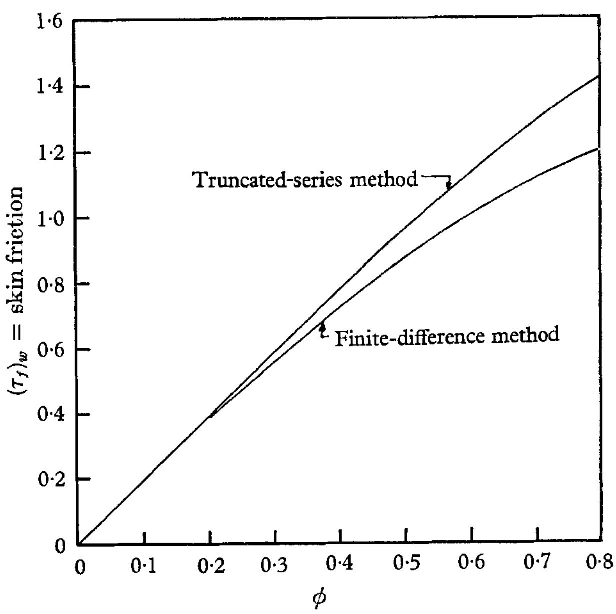

FIGURE 4(*b*). Variation of skin friction for $Re_s = 100$.

cases, however, the deviation from a spherical shock is small. This gives an indication that the assumption of a spherical shock is a good one.

Figures 3(*a*)–(*c*) show the *u*-component of velocity between the body and the shock. One can see from the figures that the results from the series-truncation method and the finite-difference method are in close agreement for small ϕ. This is what one would expect, since only one term is used in the series-truncation method. One also notices that in going to the higher Reynolds numbers one has

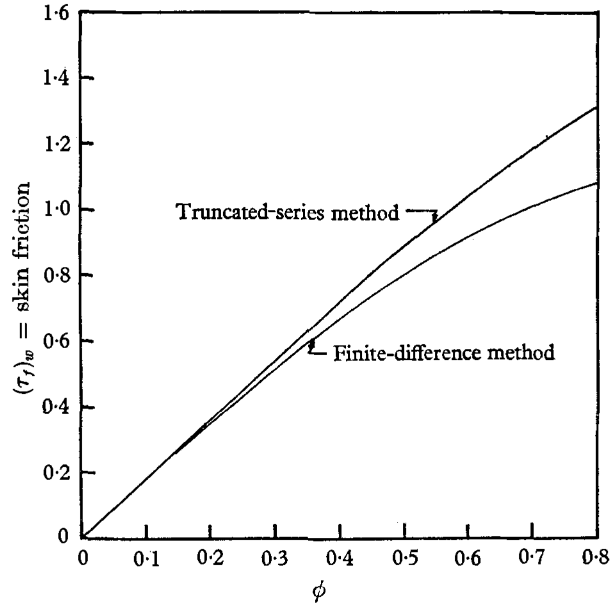

FIGURE 4(*c*). Variation of skin friction for $Re_s = 900$.

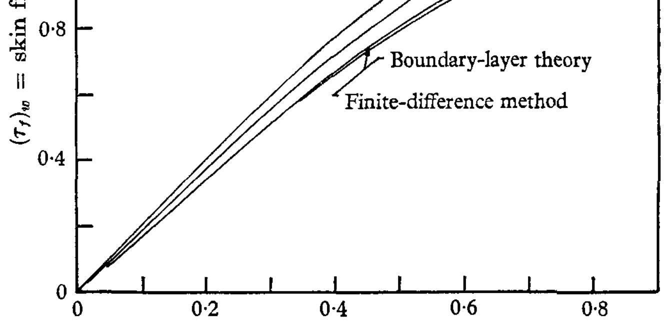

FIGURE 4(*d*). Variation of skin friction at various Reynolds numbers.

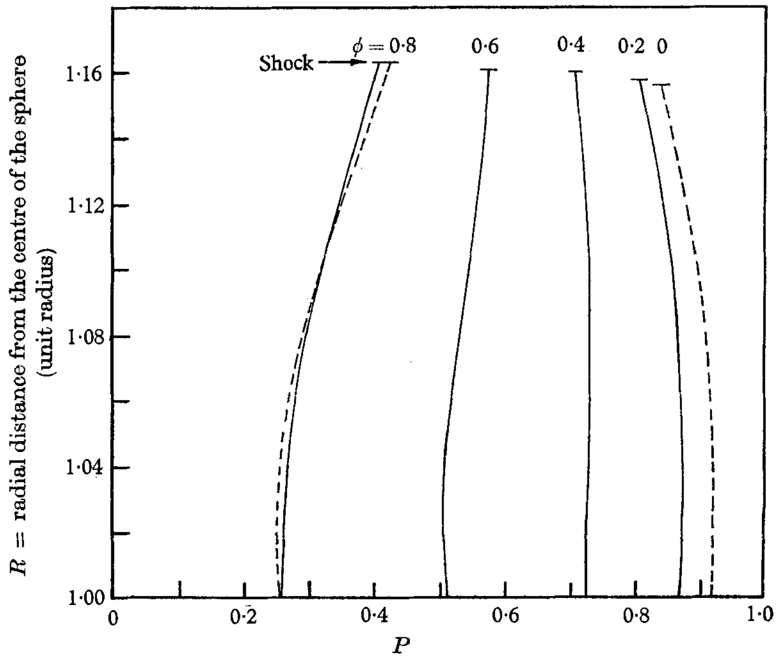

FIGURE 5(*a*). Pressure distribution for the flow with $Re_s = 49$.——, Finite-difference method; – – –, truncated-series method.

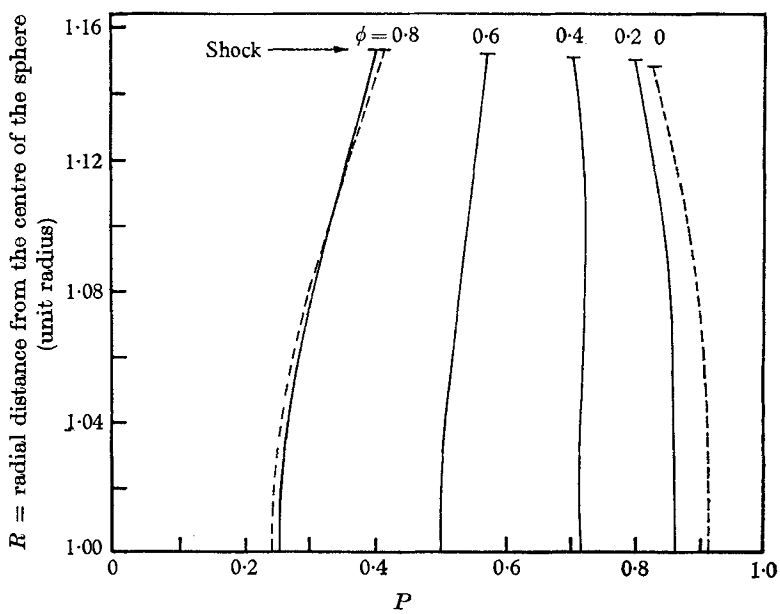

FIGURE 5(*b*). Pressure distribution for the flow with $Re_s = 100$. ——, Finite-difference method; – – – –, truncated-series method.

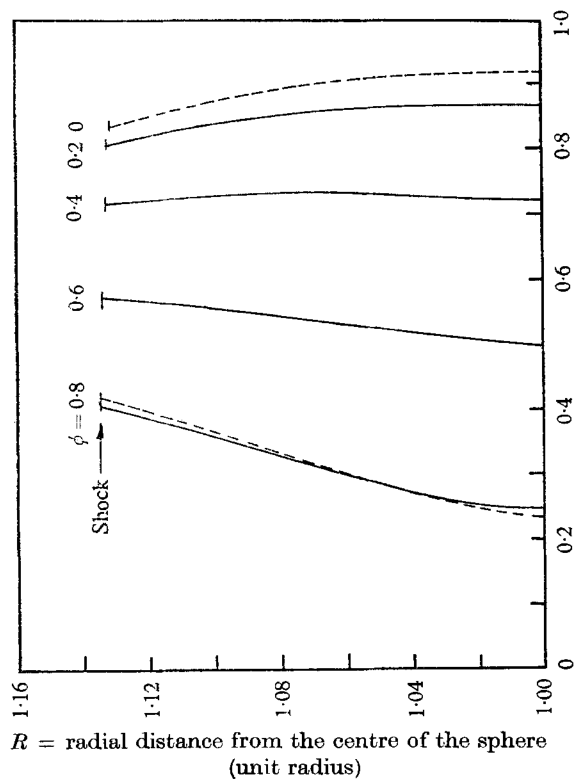

FIGURE 5(c). Pressure distribution for the flow with $Re_s = 900$. ——, Finite-difference method; – – –, truncated-series method.

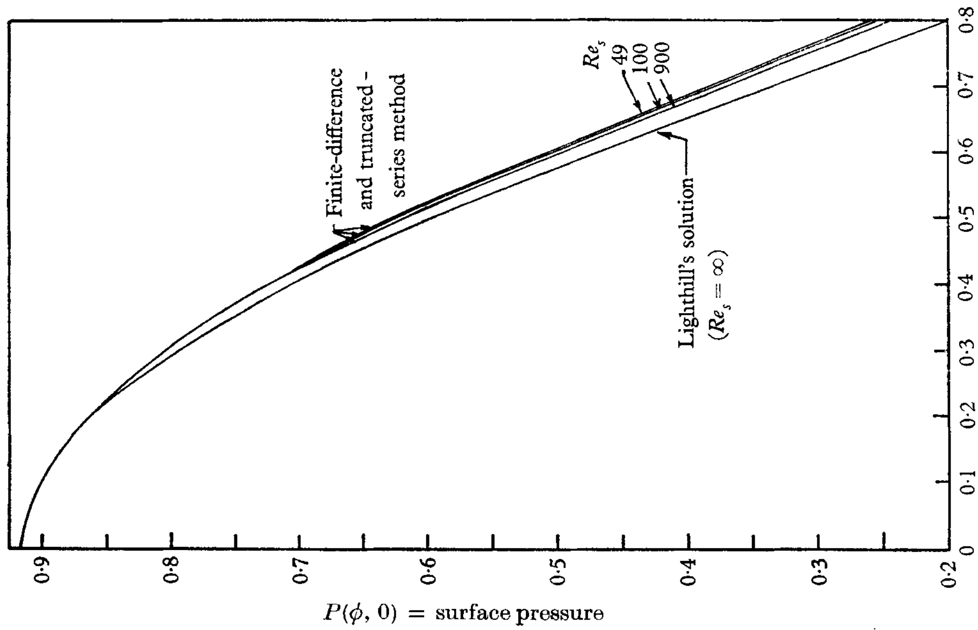

FIGURE 5(d). Variation of surface pressure along the body surface for various Reynolds numbers.

the clear indication of the formation of a boundary layer. However, even in the case of Reynolds number of 100 the indication is that the viscous effects extend over most of the shock layer. Figure 3(*c*) ($Re_s = 900$) has a comparison with Lighthill's (1957) constant-density inviscid solution. In the inviscid part of the flow field one sees that there is good agreement between the two solutions. If one includes the effect of displacement thickness to obtain the inviscid solution, one finds almost exact agreement in the inviscid region.

Figures 4(*a*)–(*d*) show the variation of skin friction over the sphere. As one would expect the truncated-series method and the finite-difference method agree well only near the stagnation point. Figure 4(*d*) shows the results from the finite-difference method for the full shock layer as compared with the finite-difference method used on the boundary-layer equations. One sees that the agreement is good at high Reynolds numbers. The boundary-layer solution was obtained by using Lighthill's (1957) constant-density solution to obtain the pressure distribution on the sphere.

Finally, figures 5(*a*)–(*d*) show pressure distributions for the flow past the sphere. Figures 5(*a*)–(*c*) show pressure distributions across the shock layer. The agreement between the truncated-series method and the finite-difference method is excellent for all positions in the shock layer. The fact that the pressure agreement between the two methods is so good is due to the fact that the pressure distribution across the viscous region (boundary layer) is essentially constant. This means that, since the form of the truncation was taken to be the same as the constant-density inviscid flow, one would expect good agreement in the pressures. Figure 5(*d*) shows the surface-pressure distribution on the sphere. The difference between the finite-difference method and truncated-series method is so slight that it cannot be detected on the plot. It can be seen that the pressure distribution is going towards Lighthill's constant-density solution as Reynolds number increases. This is as one would expect, since Lighthill's pressure distribution should be valid for infinite Reynolds number.

5. Conclusions

It has been demonstrated that it is possible to integrate numerically a set of equations valid in the entire shock layer which are an approximation to the Navier–Stokes equations for high Reynolds number. These equations are integrated by starting at the stagnation point and integrating downstream with the use of an implicit finite-difference method. The case considered was for the constant-density viscous flow past a sphere; however, the method for handling the compressible case is completely analogous. The results obtained agree with those obtained from the series-truncation solution and also with the inviscid constant-density solution of Lighthill (1957) when the Reynolds number is high enough. Effects such as shock structure and slip have not been included; however, they can be considered easily, since the numerical procedure for solving the governing equations is now clear.

In the future the method can be used for determining solutions to problems such as the flow far downstream on a hyperboloid in compressible supersonic flow. From the boundary-layer point of view it is not clear what the solution is in the region where the entropy layer and boundary layer merge. The method used here is not concerned with these difficulties since the entire shock layer is treated at once.

This research was supported in part by NASA Grant SC–NGR–47–004–006.

REFERENCES

CHENG, H. K. 1963 The blunt-body problem in hypersonic flow at low Reynolds number. *Cornell Aero. Lab. Rep.* no. AF-1285-A-10.

DAVIS, R. T. & FLÜGGE-LOTZ, I. 1964 Second-order boundary-layer effects in hypersonic flow past axisymmetric blunt bodies. *J. Fluid Mech.* **20**, 593–623.

FLÜGGE-LOTZ, I. & BLOTTNER, F. G. 1962 Computation of the compressible laminar boundary-layer flow including displacement-thickness interaction using finite-difference methods. *Div. Engng Mech., Stanford Univ., Tech. Rep.* no. 131. (Abbreviated version published in *J. Méchanique*, **2**, 397–423.)

HOFFMAN, G. H. 1964 Solution of the inviscid flow due to displacement by the method of integral relations. *Lockheed Missiles & Space Co. Tech. Rep.* no. H-64-017.

HOSHIZAKI, H. 1959 Shock-generated vorticity effects at low Reynolds number. *Lockheed Aircraft Corp., Missiles & Space Div. Rep.* no. LMSD-48381, **1**, 9–43.

KAO, H. C. 1964 Hypersonic viscous flow near the stagnation streamline of a blunt body. I. A test of local similarity. *AIAA Journal*, **2**, no. 11, 1892–1897.

LIGHTHILL, M. J. 1957 Dynamics of a dissociating gas. Part I. Equilibrium flow. *J. Fluid Mech.* **2**, 1–32.

OGUCHI, H. 1958 Flow near the forward stagnation point of a blunt body of revolution. *J. Aero/Space Sci.* **25**, 789–90.

PROBSTEIN, R. F. & KEMP, N. H. 1960 Viscous aerodynamic characteristics in hypersonic rarefied gas flow. *J. Aero/Space Sci.* **27**, 174–92.

RICHTMYER, R. D. 1957 *Difference Methods for Initial-Value Problems*. New York: Interscience.

SMITH, A. M. O. & CLUTTER, D. W. 1963 Solution of the incompressible laminar boundary-layer equations. *AIAA Journal*, **1**, no. 9, 2062–2071.

STREET, R. E. 1960 A study of boundary conditions in slip-flow aerodynamics. *Rarefied Gas Dynamics* (ed. F. M. Devienne), pp. 276–92. London: Pergamon Press.